Pionium Lifetime and $|a_0 - a_2|$ Measurement with the full DIRAC Ni Data Sample

A. Romero[1,2], B. Adeva[1], J.L. Fungueiriño Pazos[1],
O. Vázquez Doce[1,2],

[1] *IGFAE, University of Santiago de Compostela, Spain*
[2] *INFN, Istituto Nazionale di Fisica Nucleare, Frascati, Italy*

Abstract

We present in this note the final measurement of Pionium lifetime in DIRAC, from the full 2001, 2002 and 2003 Ni data samples. Including statistical and systematic error, the measurement reaches 7% precision in the lifetime and 3.5% precision in the difference of s-wave scattering lengths $|a_0 - a_2|$, and it is based upon the observation of 17005 $\pm$ 386 atom pairs. The data are shown with a single representation of the relative momentum spectra, which summarizes the separate analysis carried out for 2001 and 2002+2003 data periods. The latter are reported in a simultaneous note, in order to show their specific features.

DIRAC internal note 07-14 *2 November 2007*

1 Analysis method and corrections

1.1 Statistical analysis

We remind here the definition [1] of the χ^2 in the analysis of the prompt $2D$ spectrum in (Q_T, Q_L) plane :

$$\chi^2 = \sum_j \frac{\left(N_p^j - \beta(\alpha_1[\epsilon\frac{N_{KK}^j}{N_{KK}} + (1-\epsilon)\frac{N_{CC}^j}{N_{CC}}] - \alpha_2\frac{N_{AC}^j}{N_{AC}} - \alpha_3\frac{N_{NC}^j}{N_{NC}} - \gamma\frac{N_{AA}^j}{N_{AA}}) \right)^2}{N_p^j + \beta^2(\alpha_1^2[(1-\epsilon)^2\frac{N_{CC}^j}{N_{CC}^2} + \epsilon^2\frac{N_{KK}^j}{N_{KK}^2}] + \alpha_2^2\frac{N_{AC}^j}{N_{AC}^2} + \alpha_3^2\frac{N_{NC}^j}{N_{NC}^2} + \gamma^2\frac{N_{AA}^j}{N_{AA}^2})} \quad (1)$$

where α_i and γ are the respective Monte Carlo type fractions (constrained by $\alpha_1 + \alpha_2 + \alpha_3 + \gamma = 1$), β represents the global normalization of the Monte Carlo, which corresponds essentially to the total number of prompt events in the fit region [1] . N_p^j, N_{CC}^j, N_{AC}^j, N_{NC}^j, N_{AA}^j are the number of prompt, Coulomb, accidental, non-Coulomb and atom pairs, respectively, in each $2D$ bin, as described in our previous note [1]. Correspondingly, N_p, N_{CC}, N_{AC}, N_{NC}, N_{AA} are the total number of events in the fit region.

A control region is defined by the domain under the cut $Q_L > 2MeV/c$. We call $Q_L < 2MeV/c$ the extrapolation region. Errors are obtained by χ^2 variation of one unit. The fit strategy is to perform a preliminary fit that includes the Pionium Monte Carlo in the linear combination. Then the latter is subtracted and the difference between prompt and Monte Carlo spectra is analysed in detail, in order to measure the number of atom pairs. The breakup probability is then determined by means of the K-factors [1].

The χ^2-fit is performed either globally, including all statistics, as reported in section 2, or at ten individual pair momentum $600MeV/c$ bins, as will be seen in section 3. A detailed study of resolution with the full-tracking procedure used here was carried out in [2].

1.2 Summary of corrections

Several small corrections to the data have been reported in our previous work [1], which description we are not repeating here. Let us simply recall the status of these corrections in the present analysis:

[1] more detailed definitions will be provided in section 2

- A Q_L trigger acceptance correction is done based upon the observed behaviour of the full sample of accidental pairs, which has been described for 2001 [1] and 2002+2003 data [3]. When this correction is applied (see sections 2 and 3), genuine agreement between prompt pairs and standard Coulomb interaction background will be revealed.
- K^+K^- contamination correction is done using Monte Carlo and real data [4], [5], as explained in [1].
- the target impurity correction is done according to reference [6], as before [1].
- no finite-size correction appears to be necessary, as advanced in our previous work [1]. The significance for this is newly increased, as it will be seen below in tables 1, 8 and 9.

2 Combined global fit analysis

The global fit consists in minimizing the χ^2 defined in (1) in $2D$ with respect to α_3 (non-Coulomb fraction) and γ parameters, using the momentum-integrated sample. The α_2 and ϵ parameters remain fixed in this fit, and α_2 is determined by the direct measurement of the accidental pairs fraction from the analysis of the precision time-of-flight spectrum. ϵ is fixed to the experimentally determined K^+K^- fraction previously used in [1]. β can either be left as a free parameter, or be fixed to the total number of prompt pairs in the fit region (N_p), or to the ratio $\beta = N_p^c/f_c$ where N_p^c is the number of prompt events with $Q_L > 2MeV/c$ (control region) and f_c is the ratio between the number of Monte Carlo pairs in the control region and the total number of Monte Carlo events. These options mean small variations with respect to N_p and produce slight changes in the fit results, as indicated in table 3.

We have chosen to perform the fit in 0.25×0.25 $(MeV/c)^2$ bins in the (Q_T, Q_L) plane, for the global fit. Variations with respect to this choice are reported in table 3.

Once the fit has converged, we define the atom signal in each (i, j) bin as the difference between the prompt spectrum (with accidentals subtracted) and the Monte Carlo with the Pionium component (AA) removed. This 2D signal, which reveals the excess with respect to the calculated Coulomb interaction enhancement background, is what we call the Pionium spectrum. The atom breakup probability P_{br} is then determined [7] by means of the K-factors.

This analysis has already been carried out separately for 2001 Ni data [1] and 2002+2003 Ni data [3], and what we are going to present in the following are the combined results for the full DIRAC Ni data sample. As we did for

the partial samples, we will illustrate the various corrections by flashing the results at each correction step.

The correction sequence is defined in a cumulative way, namely:

a) use improved statistics Monte Carlo.
b) include K^+K^- correction.
c) perform the target impurity correction.
d) remove the finite-size correction.

Given the fact that the Monte Carlo simulations are slightly different for each period, we will present the combined χ^2-fit results as those of a single fit with χ^2 values and number of degrees of freedom added independently.

In table 1 we present the χ^2 values (separately in control and extrapolation regions), the number of atoms N_A, the number of Coulomb pairs in the complete fit range N_{CC}, the β parameter and the P_{br} for each option.

Table 1
Fit results for the correction options $a), b), c), d)$ indicated in the text. χ^2's in the full domain, and its restriction to the control and extrapolation regions separately, are given. Also the total number of atoms N_A and coulomb pairs N_{CC}, the β parameter and the break-up probabilities are indicated.

	a)	a+b)	a)+b)+c)	a)+b)+c)+d)
χ^2_{tot}/ndf	3222.6/3200	3215.2/3200	3215.2/3200	3198.0/3200
χ^2_{ext}/ndf	326.1/320	322.3/320	322.3/320	321.3/320
χ^2_{cont}/ndf	2896.5/2880	2892.9/2880	2892.9/2880	2876.7/2880
N_A	17250 ± 374	16562 ± 360	16562 ± 360	16814 ± 363
N_{CC}	2028303 ± 8702	1996876 ± 8552	1996876 ± 8552	1972693 ± 8468
β	2484578	2484842	2484842	2484812
P_{Br}	0.422 ± 0.010	0.411 ± 0.010	0.417 ± 0.010	0.427 ± 0.010

We recover, now enhanced, the effects that we already discussed separately. Whereas the introduction of the K^+K^- contamination [4].[5] decreases the total χ^2 by 7.4 units, the removal of the finite-size correction decreases it by 17.2 units. The combined effect of both actions decreased the total χ^2 by 24.6 units. We remark that, in agreement with our earlier findings, the finite-size correction is not wanted by the data. The statistical significance will be further enhanced when we report the momentum-dependent fit in subsection 3.1.

The K^+K^- correction introduces a better stability of the measured P_{Br} values with respect to the Q_T cut, and also a better agreement between the Q_T and Q_L series of cuts to define the atom signal, at very low Q_T and Q_L values, as it can be clearly appreciated in figure 10.

The Pionium $2D$ signal is shown in the form of lego plots in figures 8 and 9.

Table 2
Comparison of global fit results for three different choices of the β parameter definition.

	β	P_{Br}	χ^2/ndf
β all range	2486202	0.419 ± 0.010	3199.0/3200
β ($Q_L > 2MeV/c$)	2485678	0.426 ± 0.010	3198.4/3200
β free	2483534	0.430 ± 0.010	3196.1/3200

Table 3
Comparison of global fit results using two different (Q_T, Q_L) binsizes.

	β	P_{Br}	χ^2/ndf	N_A
0.25×0.25	2483534	0.430 ± 0.010	3196.1/3200	16915 ± 366
0.5×0.5	2485567	0.427 ± 0.010	751.9/800	16803 ± 366

2.1 Dependence on the Q_L upper limit

Our standard fit domain is the region $Q_L < 20MeV/c$ and $Q_T < 5MeV/c$, and the dependence of the P_{Br} with respect to the Q_L upper limit (Q_L^{up}) is analysed in table 4 and figure 1. No appreciable systematics is observed and the value at $Q_L^{up} = 20MeV/c$ is close to the average.

Table 4
Values of break-up probability P_{Br} obtained from different choices of the upper limit (Q_L^{cut}) used to define the control region in Q_L projection.

$Q_L^{cut}(MeV/c)$	P_{Br}
22	0.426 ± 0.010
21	0.430 ± 0.010
20	0.430 ± 0.010
19	0.429 ± 0.010
18	0.426 ± 0.010
17	0.426 ± 0.010
16	0.428 ± 0.011
15	0.429 ± 0.011
14	0.429 ± 0.011
13	0.424 ± 0.011

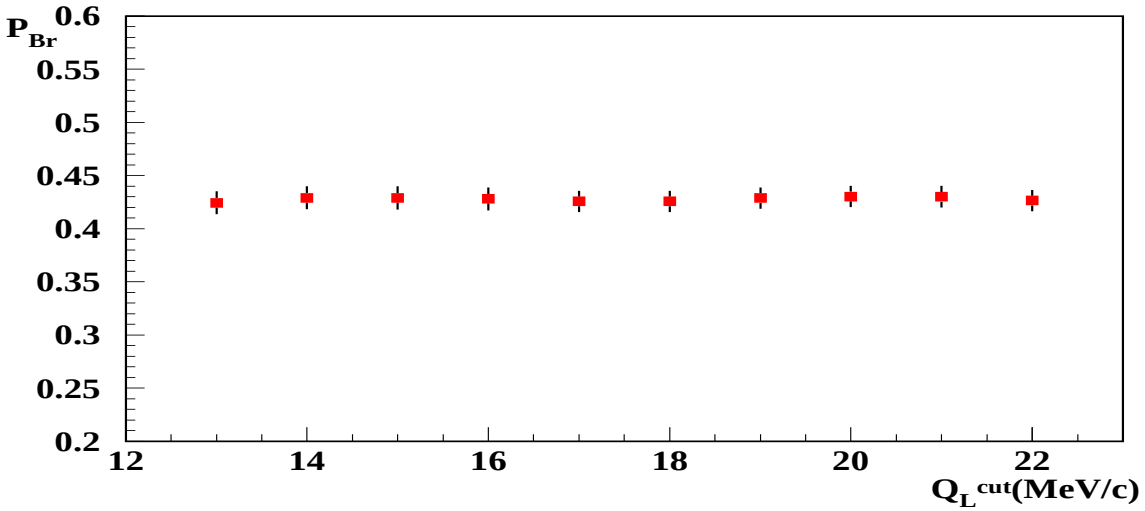

Fig. 1. *Dependence of the break-up probability on the Q_L upper cut.*

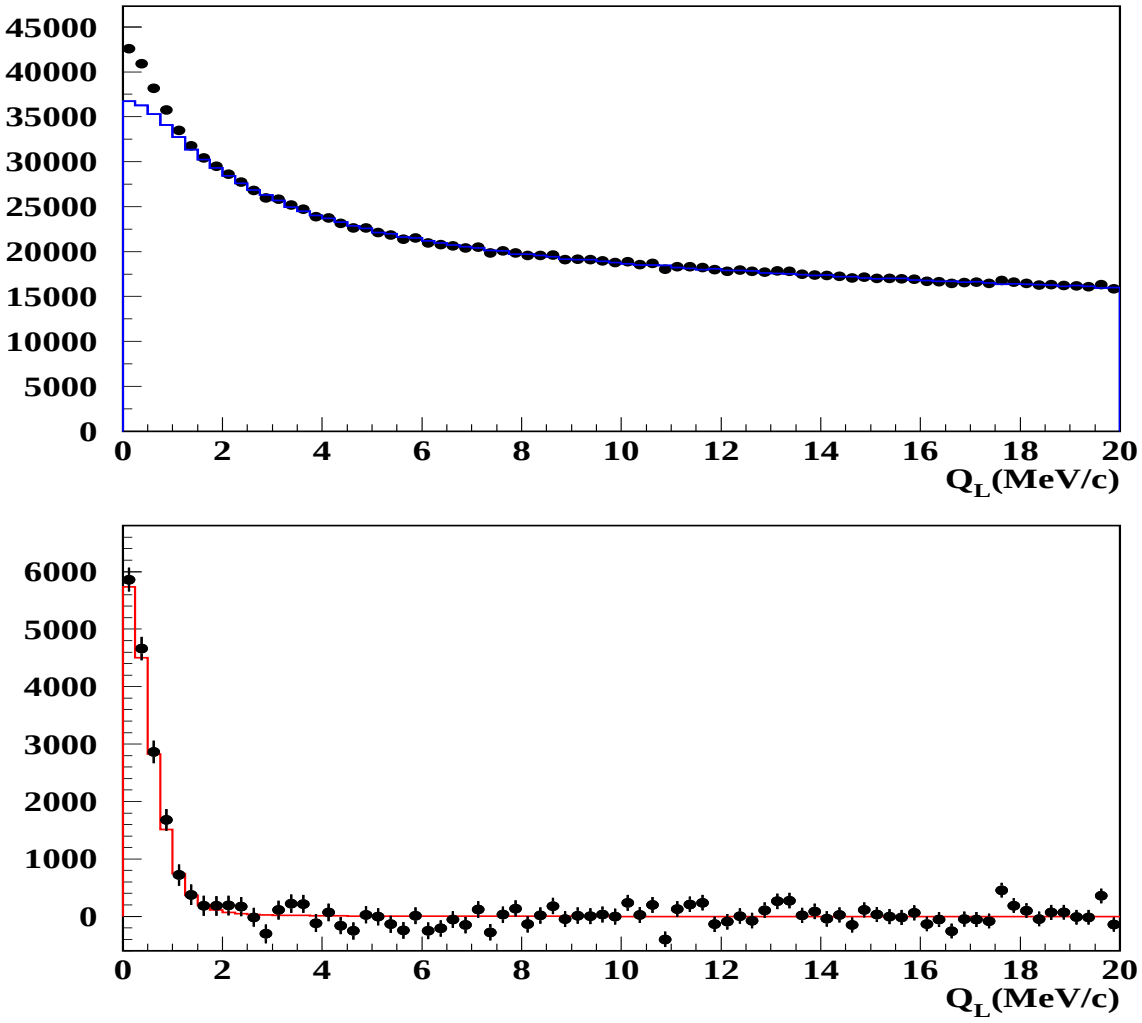

Fig. 2. *Two-dimensional global fit projection onto Q_L. The standard $Q_T < 4\ MeV/c$ cut has been applied. The difference between prompt data (dots) and Monte Carlo (blue line) , which corresponds to Pionium signal, is plotted at the bottom, where the signal is compared with the Pionium atom Monte Carlo (red line).*

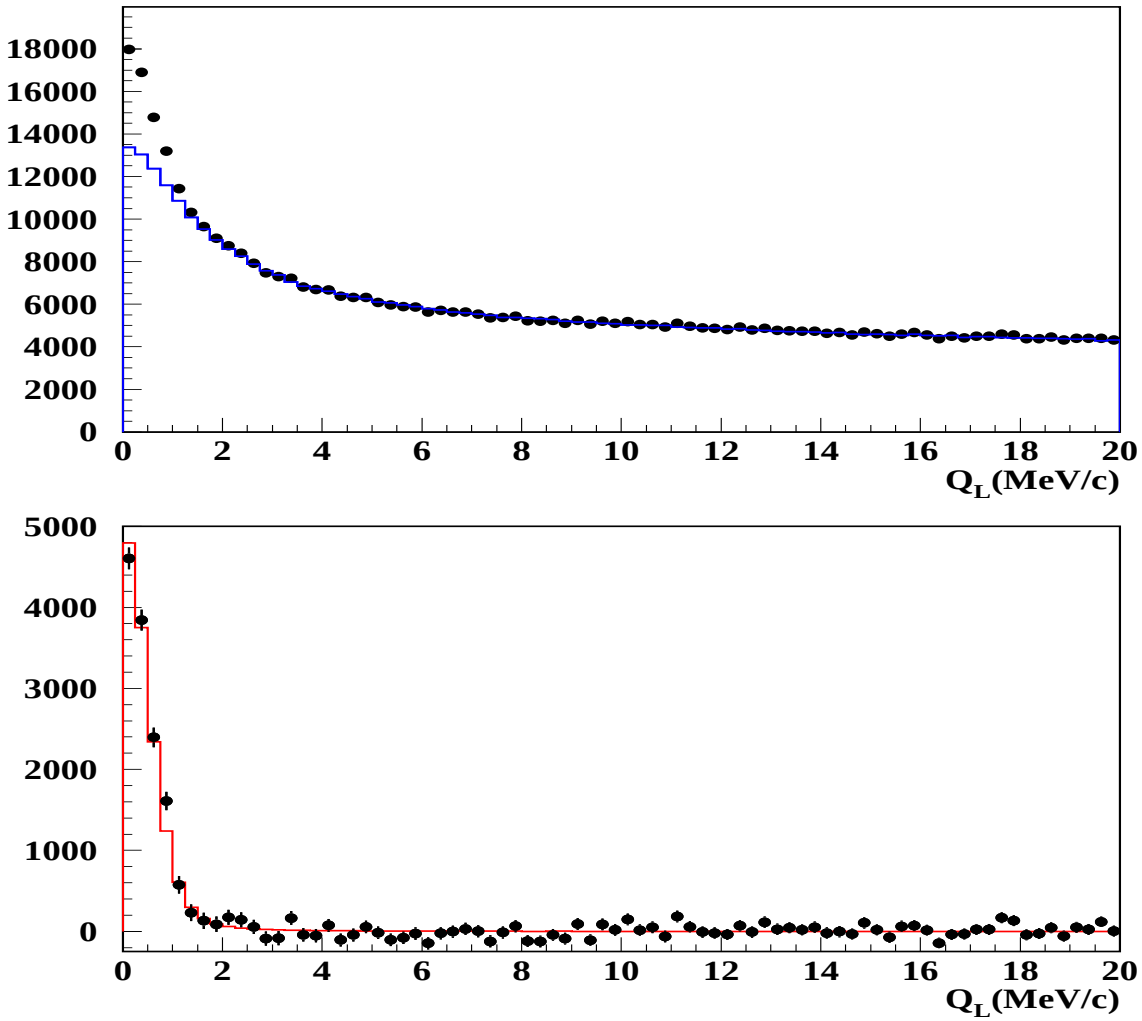

Fig. 3. *Two-dimensional global fit projection onto Q_L. A more restrictive $Q_T < 2$ MeV/c cut has been applied to enhance the signal. The difference between prompt data (dots) and Monte Carlo (blue line) , which corresponds to Pionium signal, is plotted at the bottom, where the signal is compared with the Pionium atom Monte Carlo (red line).*

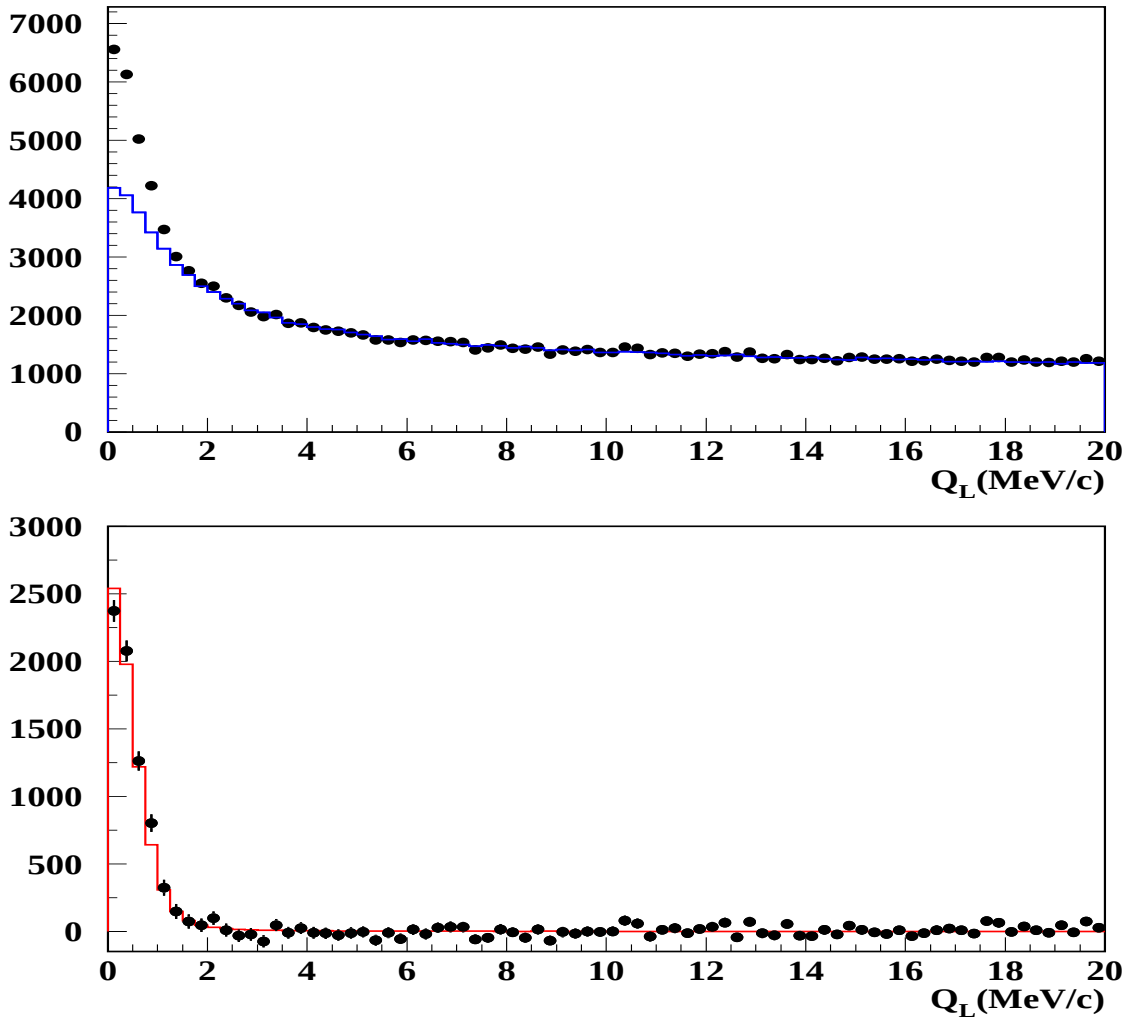

Fig. 4. *Two-dimensional global fit projection onto Q_L. A more restrictive $Q_T < 1$ MeV/c cut has been applied to enhance the signal. The difference between prompt data (dots) and Monte Carlo (blue line) , which corresponds to Pionium signal, is plotted at the bottom, where the signal is compared with the Pionium atom Monte Carlo (red line).*

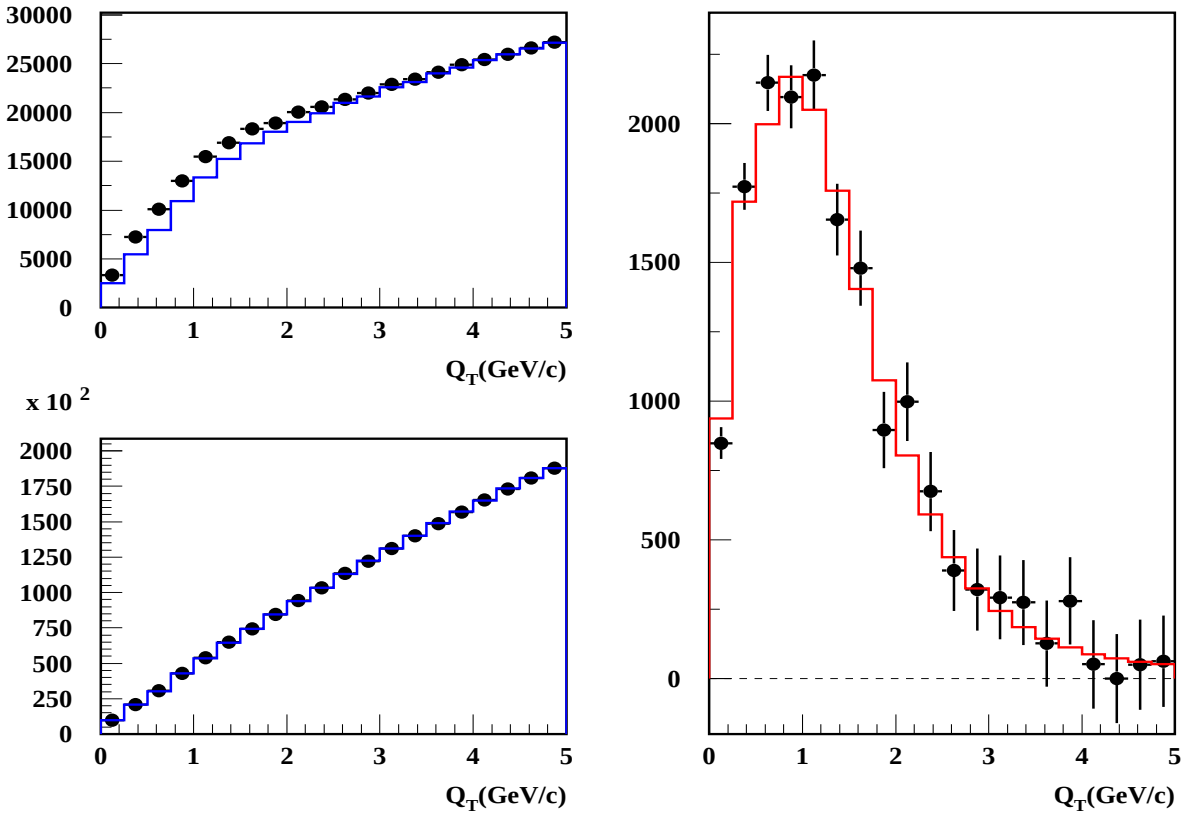

Fig. 5. *Two-dimensional global fit projection onto Q_T. The data are shown separately for $Q_L < 2MeV/c$ (left top) and $Q_L > 2MeV/c$ (left bottom). The difference between prompt data (dots) and Monte Carlo (blue line), which corresponds to transverse Pionium signal, is plotted (right) and compared with the Pionium atom Monte Carlo (red line).*

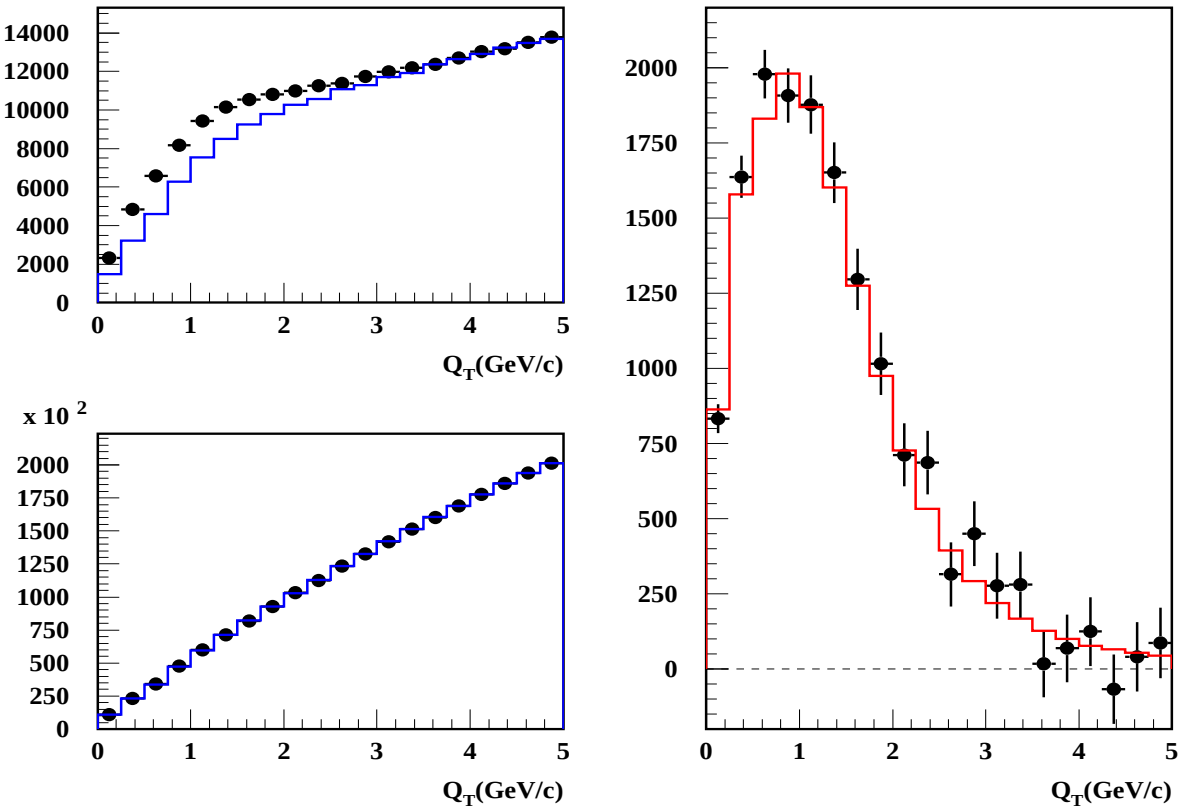

Fig. 6. *Two-dimensional global fit projection onto Q_T. The data are shown separately for $Q_L < 1MeV/c$ (left top) and $Q_L > 1MeV/c$ (left bottom). The difference between prompt data (dots) and Monte Carlo (blue line), which corresponds to transverse Pionium signal, is plotted (right) and compared with the Pionium atom Monte Carlo (red line).*

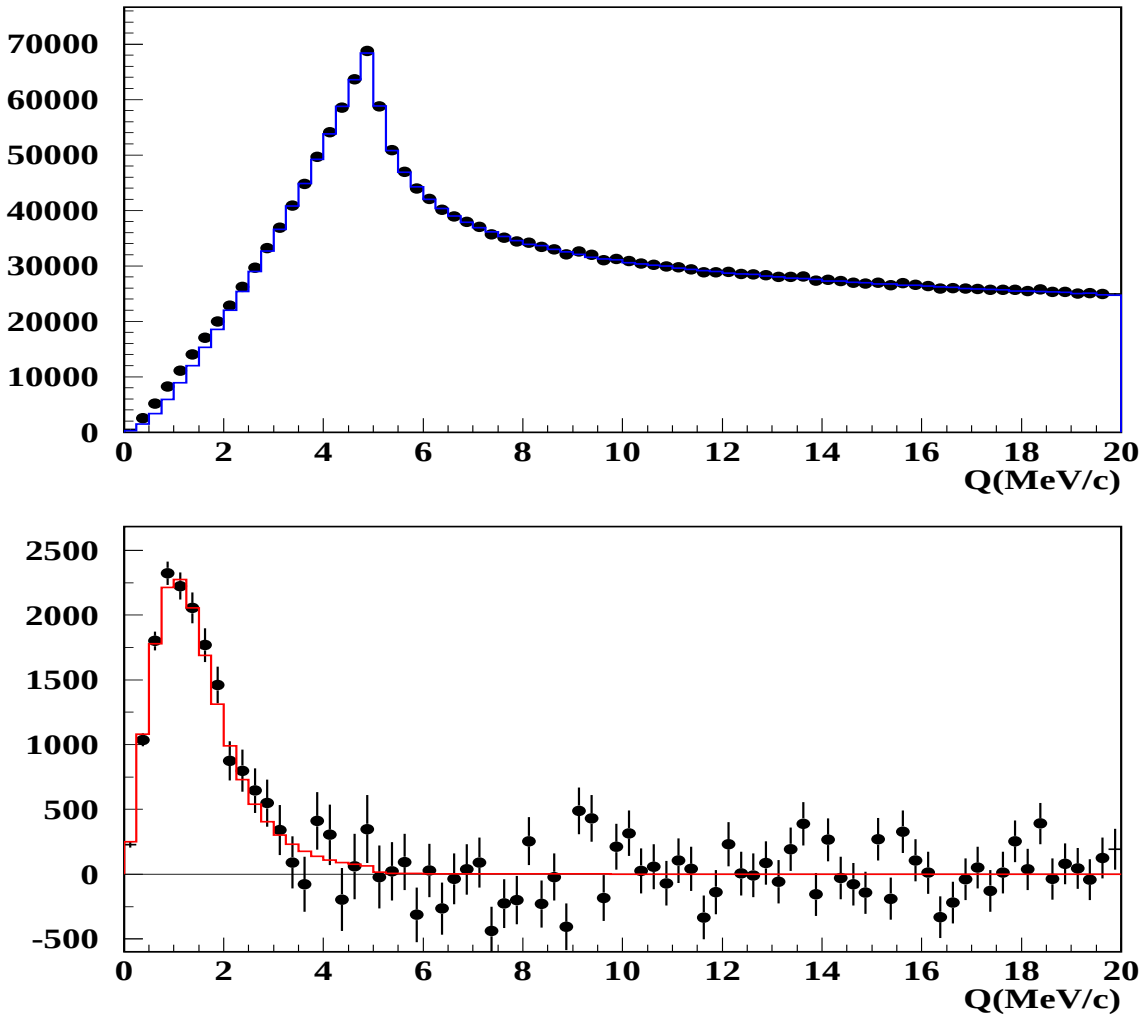

Fig. 7. *Two-dimensional global fit projection onto Q. The standard $Q_T < 4MeV/c$ cut was applied. The difference between prompt data (dots) and Monte Carlo (blue line) , which corresponds to Pionium signal, is plotted at the bottom. The signal is compared with the Pionium atom Monte Carlo (red line).*

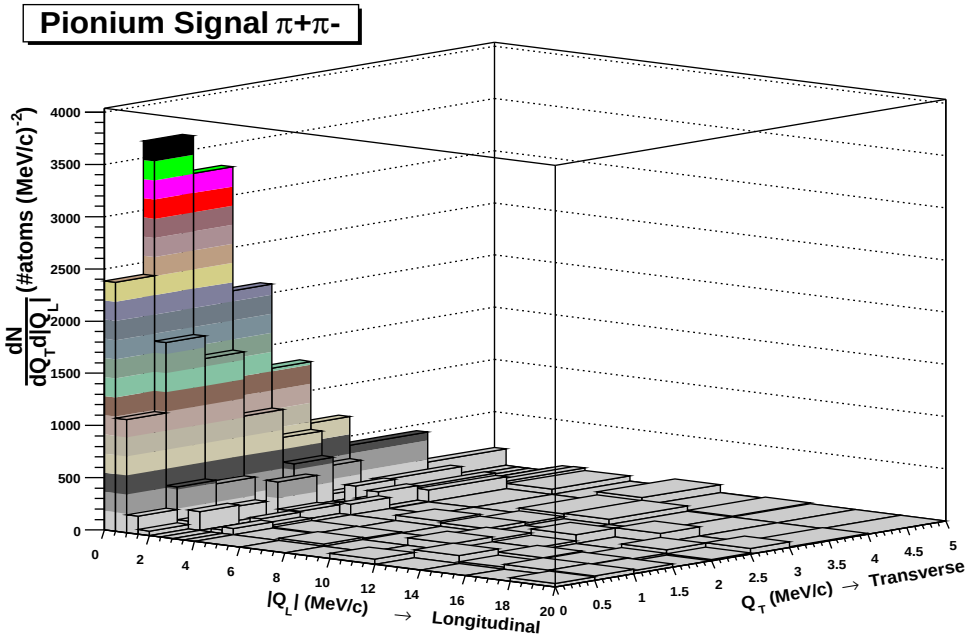

Fig. 8. *Lego plot showing the Pionium break-up spectrum in Ni in the* $(Q_T, Q_L = |Q_Z|)$ *plane, after subtraction of the Coulomb background.*

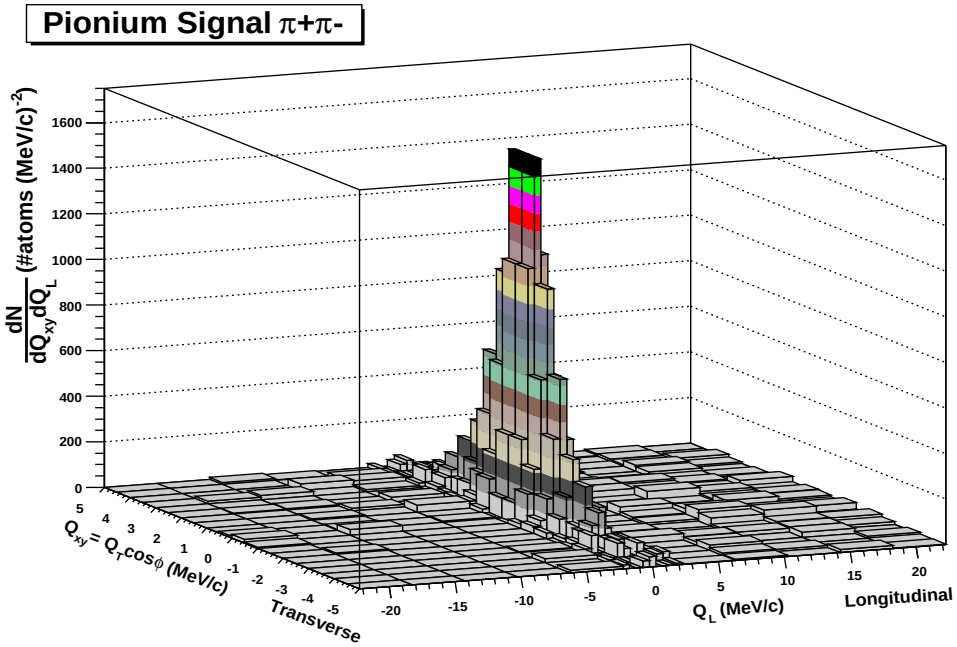

Fig. 9. *Lego plot showing the Pionium break-up spectrum in Ni in the* (Q_{xy}, Q_L) *plane, after subtraction of Coulomb background. The transverse component* $Q_{xy} = Q_T\, cos\phi$ *is defined as the product of the measured* Q_T *value times the cosine of a random azimuth.*

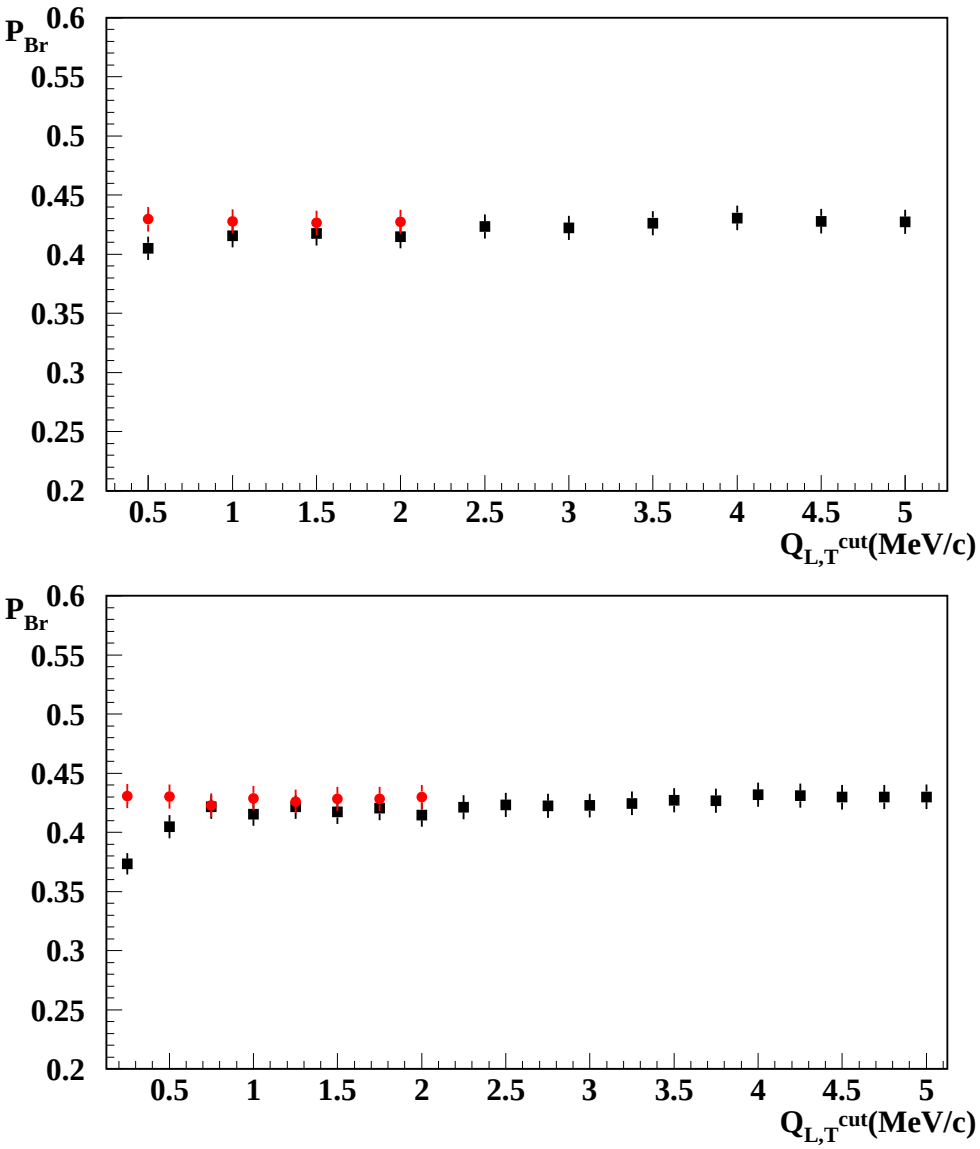

Fig. 10. *Pionium break-up probabilities determined from different choices of the upper limits ($Q^u_{T,L}$) in the rectangular integration domain to define the atom signal. Top plot shows the 2001+2002+2003 results after the introduction of K^+K^- correction, in $0.5 MeV/c$ steps of Q^u_L (red dots) and Q^u_T (black squares). Bottom plot shows the same in $0.25 MeV/c$ steps.*

3 Momentum-dependent analysis

Following the approach of our earlier work [7], in this section we split the pair momentum spectrum in ten 600 MeV/c bins and perform independent fits at each momentum interval. The corrections applied are the same as for the global fit. The only change with respect to the latter is the choice of $0.5 \times 0.5(MeV/c)^2$ binsize, which is now obliged due to the strong statistics reduction at individual 2D bins.

We shall keep track of the results at each correction step as follows:

a) Table 6: The standard Monte Carlo is used.
b) Table 7: K^+K^- contamination is introduced, after the parametrization given in [1].
c) Table 8: Standard Monte Carlo, K^+K^- contamination and target impurity correction.
d) Table 9: In addition to the above, the finite-size correction is dropped.This is the final result.

Figures from 11 to 20 show the result of the 10 independent fits in the form of atom spectra (Q_L and Q_T) and break-up probabilities as function of Q_L and Q_T cuts.

The signal line-shape shows good agreement with the Pionium Monte Carlo simulation [8],[9].

In table 5 a new global χ^2 has been defined as the sum of the individual ones at each momentum bin, and a combined P_{Br} value and error have been calculated after proper account of the independent statistical errors. The sum has been further extended to include the independent 2001 and 2002+2003 data samples. The number of atoms (N_A) and Coulomb pairs (N_C) are also indicated.

Table 5
Combined momentum dependent fit, for progressive fit conditions as defined in the text.

	A	A+B	A+B+C	A+B+C+D
χ^2	6926.0/7047	6913.4/7047	6913.4/7047	6877.4/7047
P_{Br}	0.424 ± 0.011	0.417 ± 0.010	0.423 ± 0.010	0.432 ± 0.010
N_A	17401 ± 394	16835 ± 384	16835 ± 384	17005 ± 386
N_C	1601446 ± 7252	1578030 ± 7154	1578030 ± 7154	1560276 ± 7092

From table 5 we draw the same conclusions as from the global analysis. The introduccion of K^+K^- simulation improves the χ^2 by 12.6 units, and when the finite-size correction is removed, the χ^2 improves by 36.0 additional units. We consider this a clear indication that the latter should be done. Adding this two changes, the χ^2 is reduced by 48.6 units.

Table 6

Results of the momentum-dependent fit, using correction a) only (see text). Break-up probability values P_{Br}, number of atom pairs N_A, α_1 and χ^2 over the entire fit region are indicated in this table, for every 600 MeV/c momentum interval p_i.

	P_{Br}	N_A	α_1	χ^2 /ndf	χ^2_e / ndf
p_1	0.392 ± 0.027	2094 ± 130	0.789 ± 0.013	614.2 / 648	71.8 / 72
p_2	0.433 ± 0.023	3798 ± 177	0.804 ± 0.007	638.9 / 648	81.1 / 72
p_3	0.400 ± 0.022	3158 ± 160	0.816 ± 0.008	634.3 / 648	55.2 / 72
p_4	0.436 ± 0.026	2779 ± 147	0.831 ± 0.009	601.8 / 648	72.2 / 72
p_5	0.424 ± 0.031	2080 ± 141	0.848 ± 0.011	613.2 / 648	52.1 / 72
p_6	0.445 ± 0.037	1491 ± 108	0.816 ± 0.013	692.5 / 648	64.9 / 72
p_7	0.462 ± 0.055	944 ± 996	0.824 ± 0.018	670.9 / 648	77.0 / 72
p_8	0.621 ± 0.108	623 ± 110	0.777 ± 0.025	631.9 / 642	112.6 / 72
p_9	0.571 ± 0.105	303 ± 53	0.838 ± 0.018	617.9 / 615	71.5 / 72
p_{10}	0.764 ± 0.228	154 ± 64	0.742 ± 0.046	480.7 / 534	71.2 / 72

Table 7
Results of the momentum-dependent fit, using corrections a+b (see text). Break-up probability values P_{Br}, number of atom pairs N_A, α_1 and χ^2 over the entire fit region are indicated in this table, for every 600 MeV/c momentum interval p_i.

	P_{Br}	N_A	α_1	χ^2 /ndf	χ^2_e / ndf
p_1	0.390 ± 0.027	2070 ± 128	0.786 ± 0.013	614.8 / 648	72.0 / 72
p_2	0.429 ± 0.022	3741 ± 175	0.800 ± 0.007	638.4 / 648	81.9 / 72
p_3	0.395 ± 0.022	3080 ± 156	0.811 ± 0.008	634.3 / 648	56.4 / 72
p_4	0.428 ± 0.026	2684 ± 143	0.824 ± 0.009	601.8 / 648	71.9 / 72
p_5	0.411 ± 0.031	1983 ± 137	0.840 ± 0.011	611.2 / 648	50.0 / 72
p_6	0.430 ± 0.036	1411 ± 103	0.804 ± 0.013	691.8 / 648	63.0 / 72
p_7	0.458 ± 0.055	907 ± 96	0.810 ± 0.017	670.6 / 648	74.8 / 72
p_8	0.607 ± 0.107	588 ± 105	0.763 ± 0.024	630.5 / 642	110.0 / 72
p_9	0.522 ± 0.100	269 ± 48	0.821 ± 0.025	618.2 / 615	70.8 / 72
p_{10}	0.774 ± 0.238	140 ± 66	0.665 ± 0.058	480.3 / 534	70.9 / 72

Table 8
Fit results of the momentum-dependent fit, using corrections a+b+c (see text). Break-up probability values P_{Br}, number of atom pairs N_A, α_1 and χ^2 over the entire fit region are indicated in this table, for every 600 MeV/c momentum interval p_i.

	P_{Br}	N_A	α_1	χ^2 /ndf	χ^2_e / ndf
p_1	0.395 ± 0.027	2070 ± 128	0.786 ± 0.013	614.8 / 648	72.0 / 72
p_2	0.436 ± 0.022	3741 ± 175	0.800 ± 0.007	638.4 / 648	81.9 / 72
p_3	0.402 ± 0.023	3080 ± 156	0.811 ± 0.008	634.3 / 648	56.4 / 72
p_4	0.433 ± 0.026	2684 ± 143	0.824 ± 0.009	601.8 / 648	71.9 / 72
p_5	0.417 ± 0.031	1983 ± 137	0.840 ± 0.011	611.2 / 648	50.0 / 72
p_6	0.437 ± 0.036	1411 ± 103	0.804 ± 0.013	691.8 / 648	63.0 / 72
p_7	0.465 ± 0.055	907 ± 96	0.810 ± 0.017	670.6 / 648	74.8 / 72
p_8	0.615 ± 0.108	588 ± 105	0.763 ± 0.024	630.5 / 642	110.0 / 72
p_9	0.530 ± 0.102	269 ± 48	0.822 ± 0.025	618.2 / 615	70.8 / 72
p_{10}	0.785 ± 0.242	140 ± 66	0.841 ± 0.109	480.3 / 534	70.9 / 72

Table 9
Final fit results of the momentum-dependent fit, using all corrections a+b+c+d (see text). Break-up probability values P_{Br}, number of atom pairs N_A, α_1 and χ^2 over the entire fit region are indicated in this table, for every 600 MeV/c momentum interval p_i.

	P_{Br}	N_A	α_1	χ^2 /ndf	χ^2_e / ndf
p_1	0.404 ± 0.028	2098 ± 129	0.777 ± 0.013	611.5 / 648	71.7 / 72
p_2	0.445 ± 0.023	3794 ± 176	0.790 ± 0.007	634.8 / 648	81.8 / 72
p_3	0.410 ± 0.023	3125 ± 158	0.801 ± 0.008	631.5 / 648	55.8 / 72
p_4	0.442 ± 0.026	2715 ± 144	0.816 ± 0.010	598.8 / 648	71.8 / 72
p_5	0.425 ± 0.031	2005 ± 137	0.831 ± 0.011	608.2 / 648	49.8 / 72
p_6	0.443 ± 0.037	1422 ± 104	0.796 ± 0.013	688.0 / 648	62.9 / 72
p_7	0.470 ± 0.056	910 ± 96	0.802 ± 0.017	667.4 / 648	74.3 / 72
p_8	0.615 ± 0.108	583 ± 105	0.756 ± 0.024	626.9 / 642	109.1 / 72
p_9	0.504 ± 0.099	257 ± 47	0.811 ± 0.029	614.4 / 615	70.6 / 72
p_{10}	0.742 ± 0.231	133 ± 67	0.840 ± 0.111	477.6 / 534	70.7 / 72

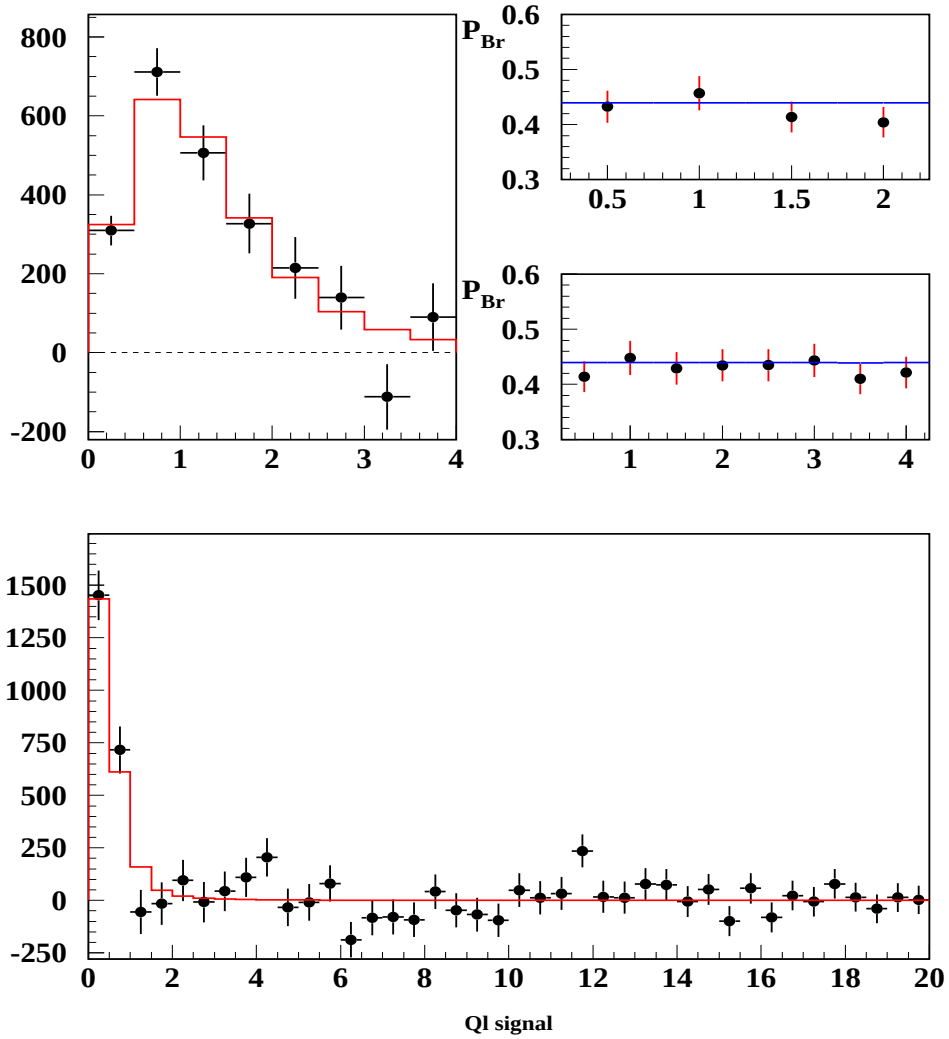

Fig. 11. *Fit results for the $\pi^+\pi^-$ momentum bin $2.6 < p < 3.2$ GeV/c in lab-frame. Q_T (top left) and Q_L (botom) projections of the atom signal found in the extrapolation region ($Q_L < 2MeV/c$) after subtraction of the Monte Carlo prediction with Pionium component removed. Values of break-up probability determined for different integration upper limits Q_T^u and Q_L^u to define the atom signal (top right). Note the different Q_L^u values are all defined for $Q_T^u = 5MeV/c$ and Q_T^u values are defined for $Q_L^u = 2MeV/c$. The blue line indicates the P_{Br} determined from atom counting using the Monte Carlo.*

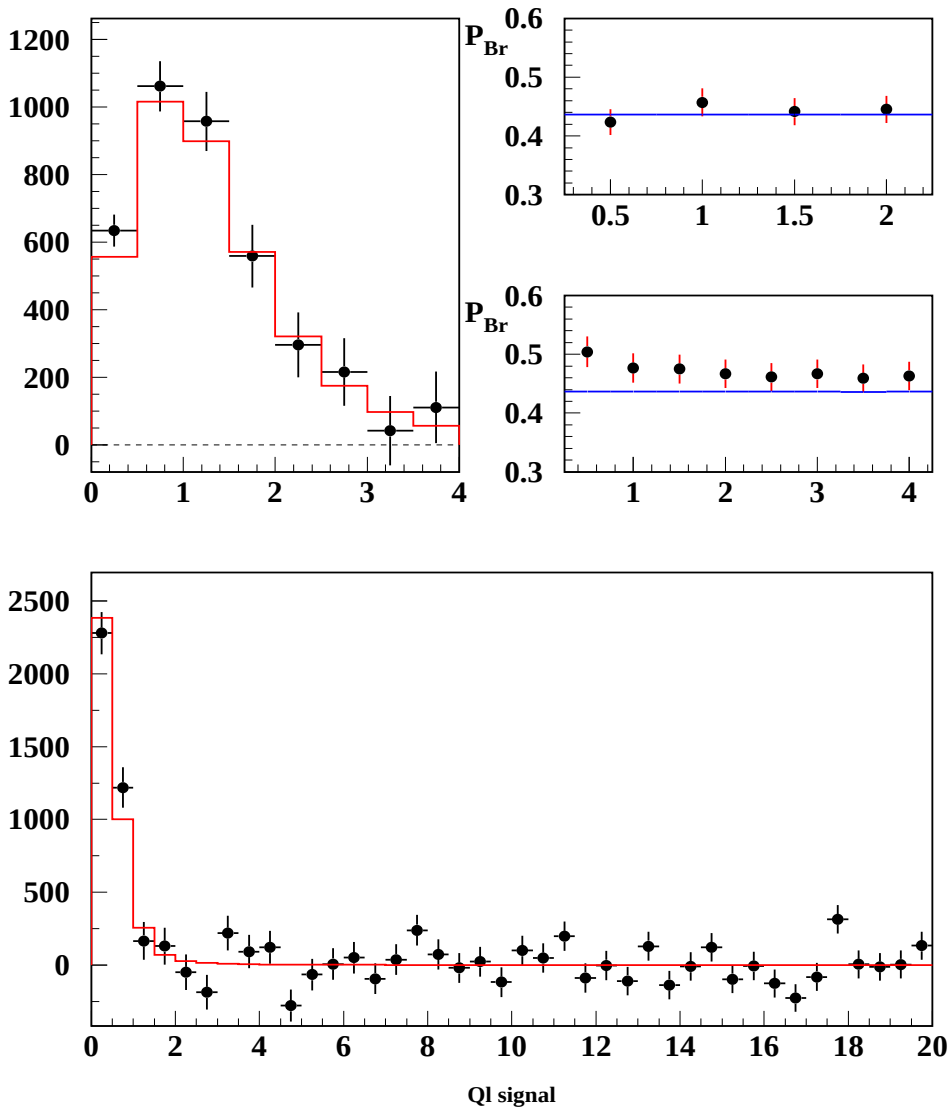

Fig. 12. *Fit results for the* $\pi^+\pi^-$ *momentum interval* $3.2 < p < 3.8$ *GeV/c in lab-frame. Caption is identical to figure 11 for the rest.*

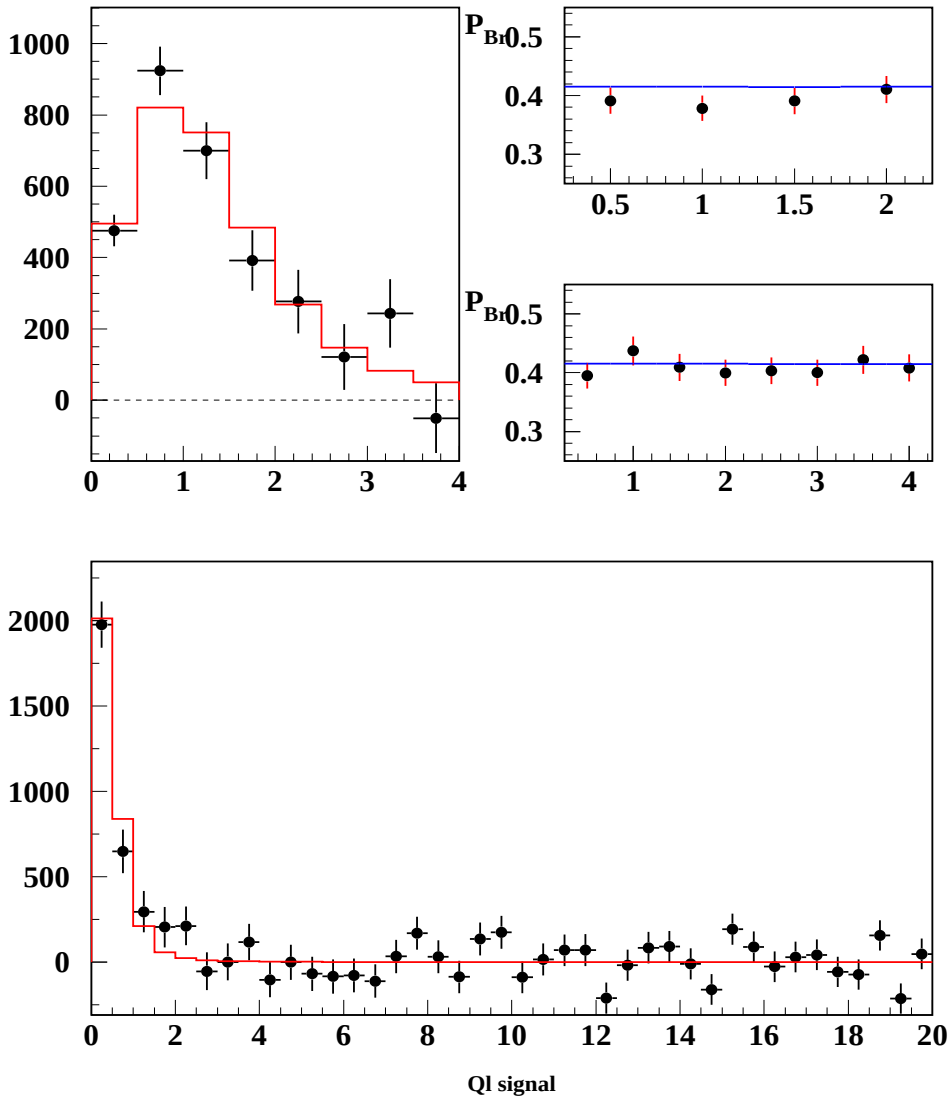

Fig. 13. *Fit results for the* $\pi^+\pi^-$ *momentum interval* $3.8 < p < 4.4$ *GeV/c in lab-frame. Caption is identical to figure 11 for the rest.*

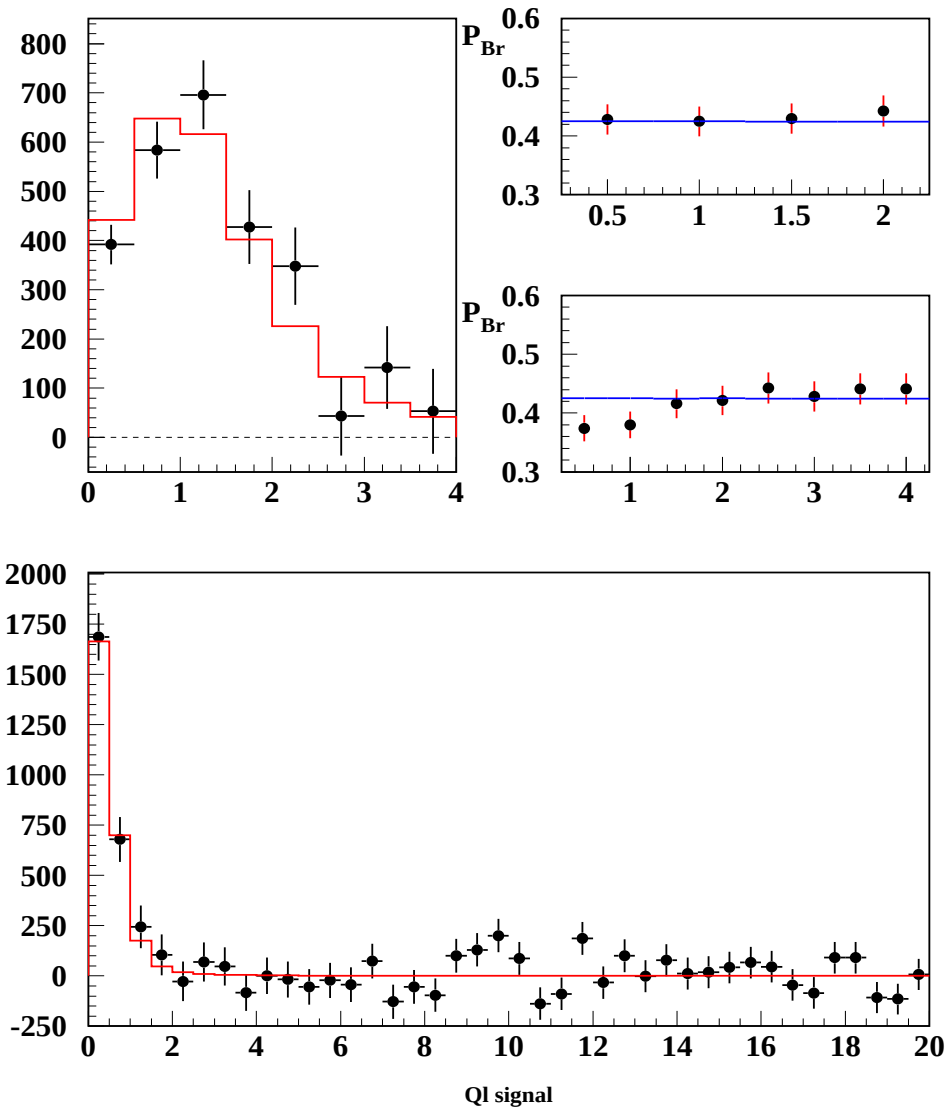

Fig. 14. *Fit results for the* $\pi^+\pi^-$ *momentum interval* $4.4 < p < 5.0$ *GeV/c in lab-frame. Caption is identical to figure 11 for the rest.*

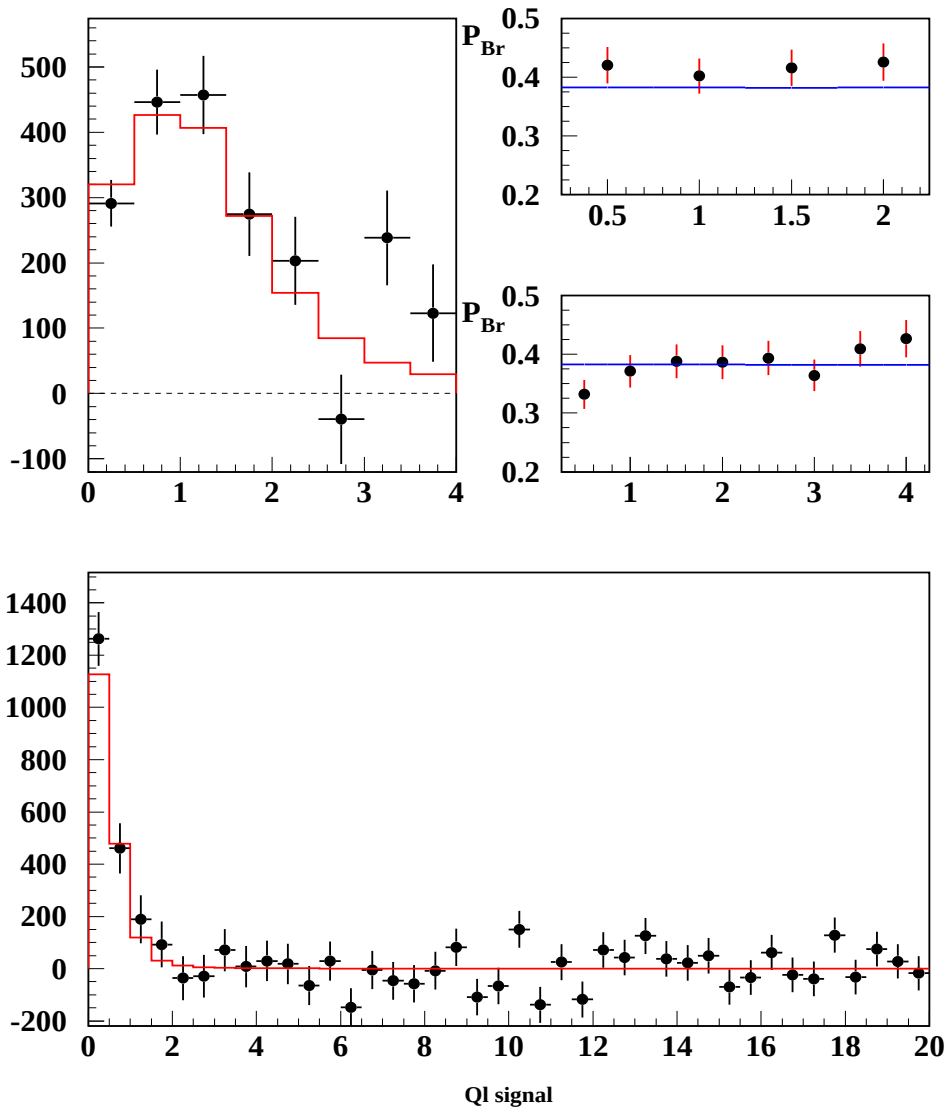

Fig. 15. *Fit results for the* $\pi^+\pi^-$ *momentum interval* $5. < p < 5.6$ *GeV/c in lab-frame. Caption is identical to figure 11 for the rest.*

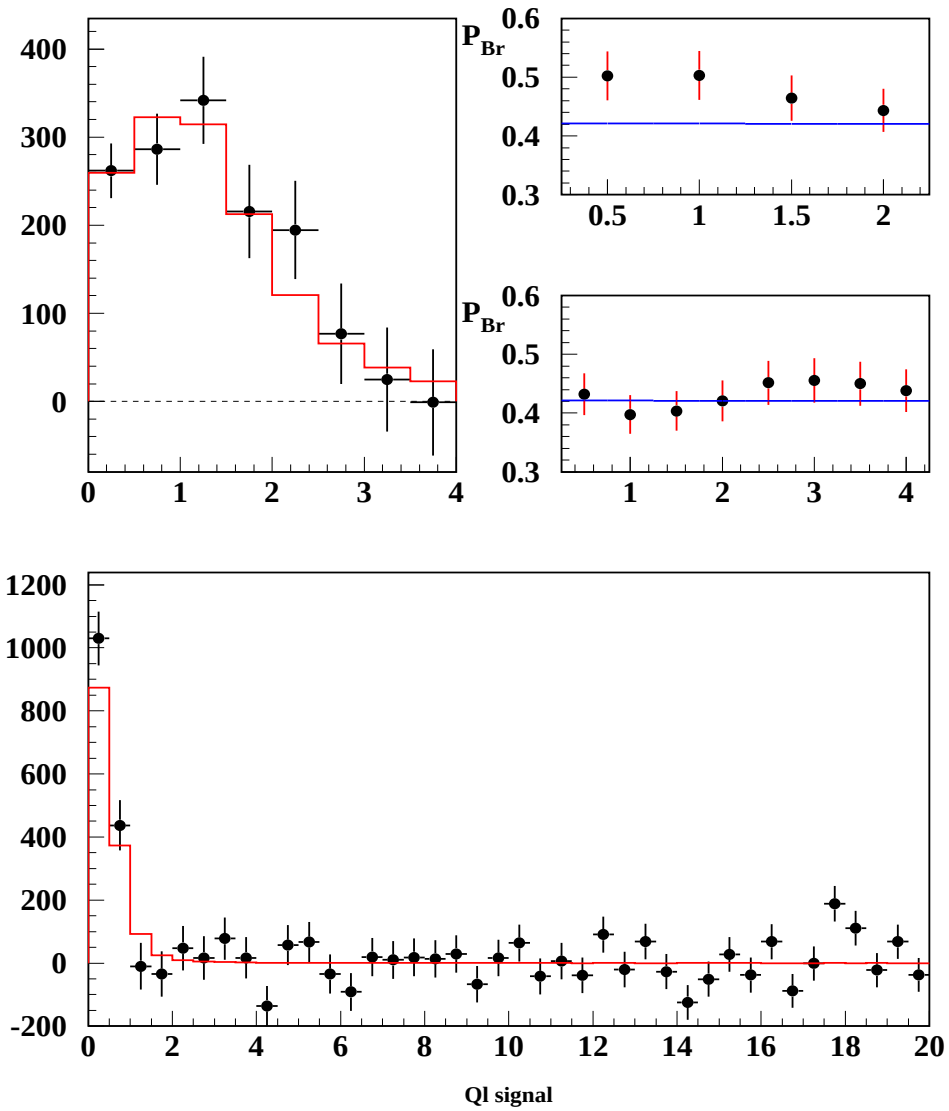

Fig. 16. *Fit results for the* $\pi^+\pi^-$ *momentum interval* $5.6 < p < 6.2$ *GeV/c in lab-frame. Caption is identical to figure 11 for the rest.*

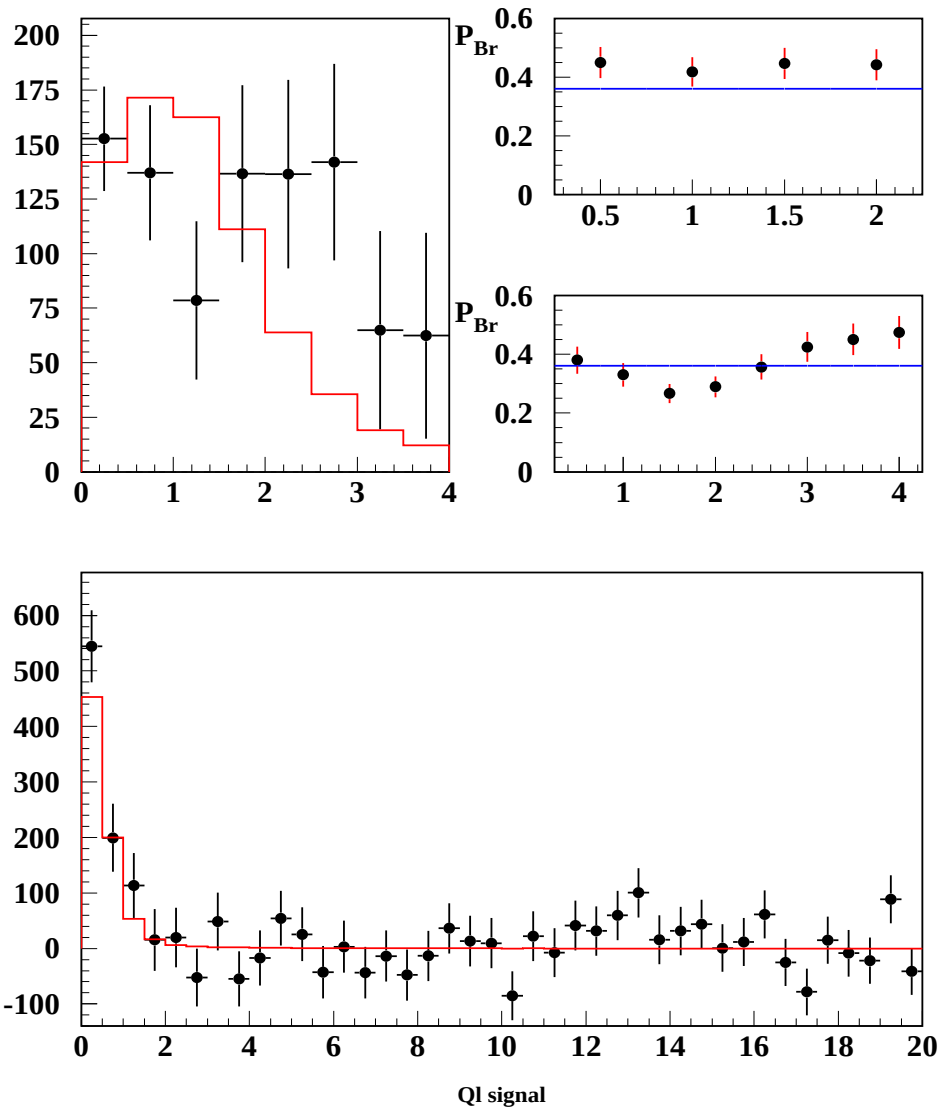

Fig. 17. *Fit results for the $\pi^+\pi^-$ momentum interval* $6.2 < p < 6.8$ *GeV/c in lab-frame. Caption is identical to figure 11 for the rest.*

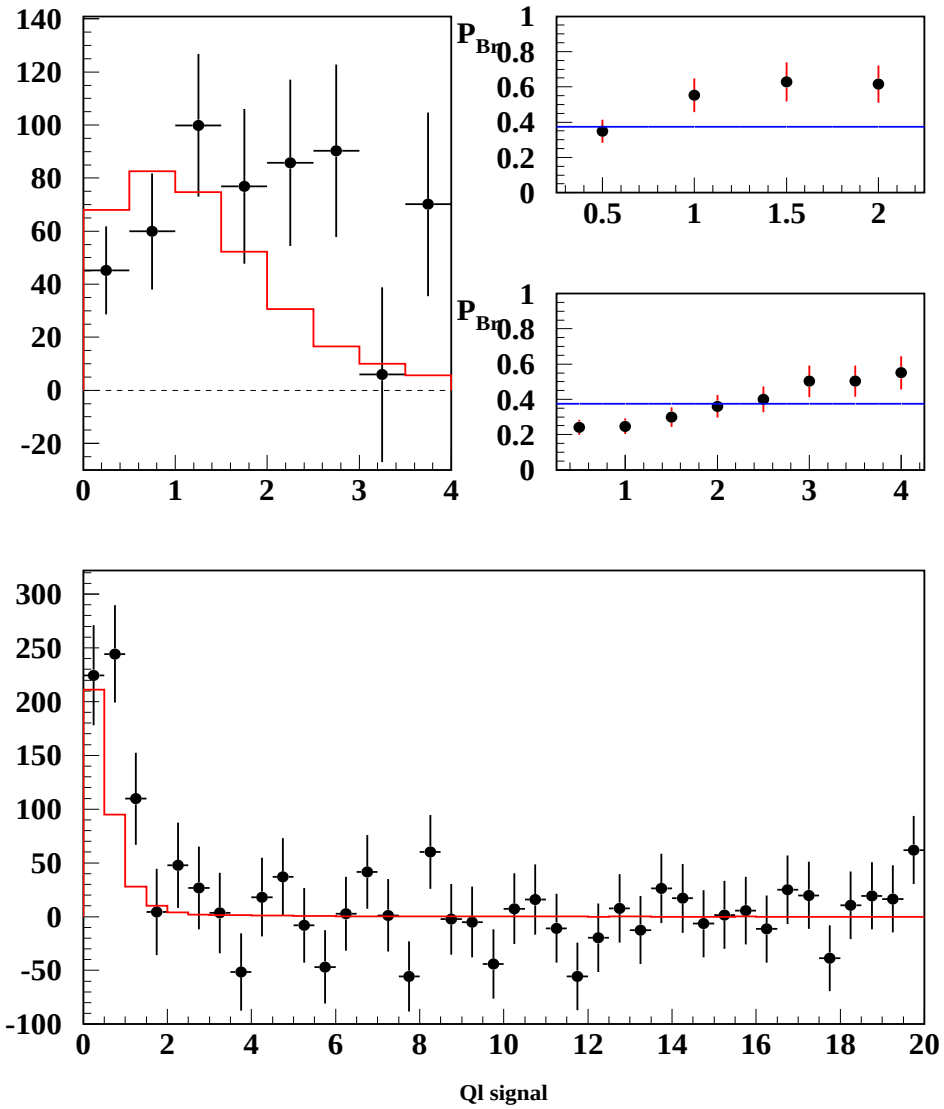

Fig. 18. *Fit results for the* $\pi^+\pi^-$ *momentum interval* $6.8 < p < 7.4$ *GeV/c in lab-frame. Caption is identical to figure 11 for the rest.*

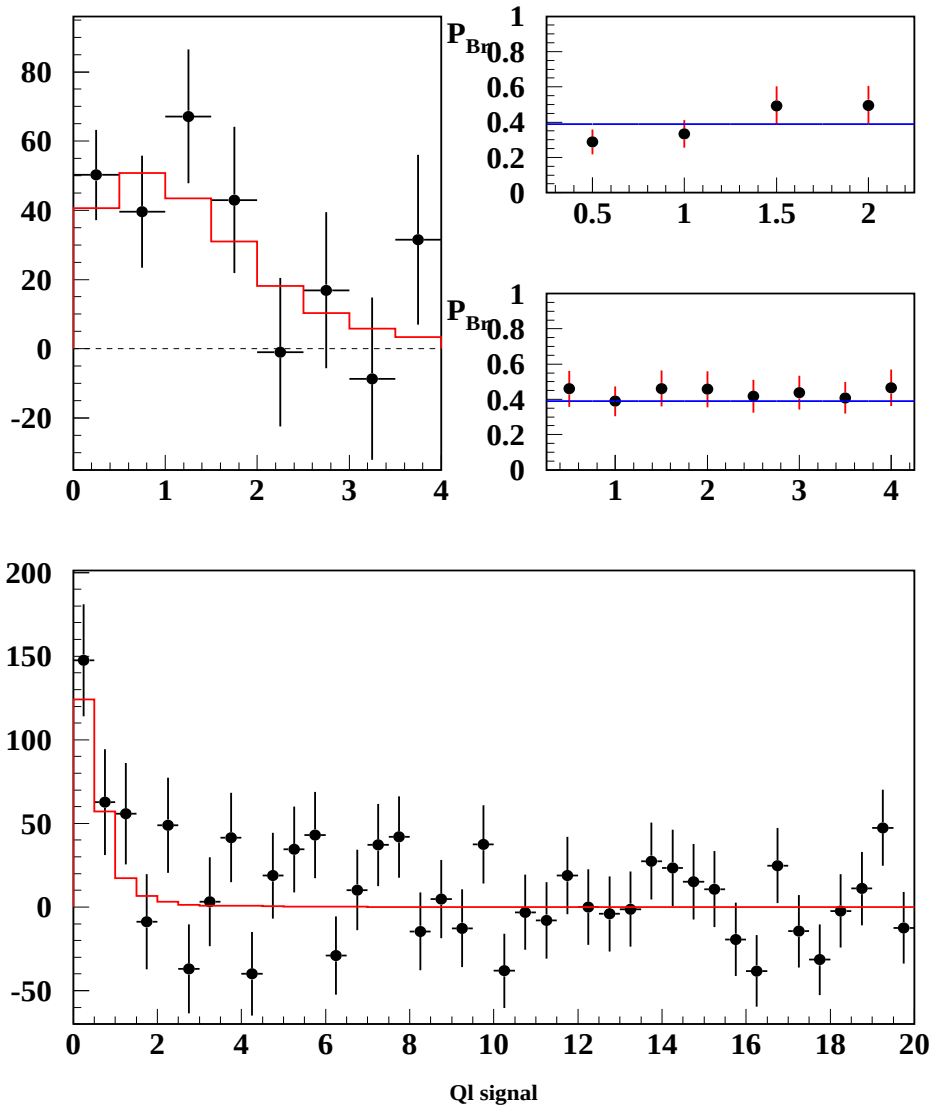

Fig. 19. *Fit results for the $\pi^+\pi^-$ momentum interval $7.4 < p < 8.0$ GeV/c in lab-frame. Caption is identical to figure 11 for the rest.*

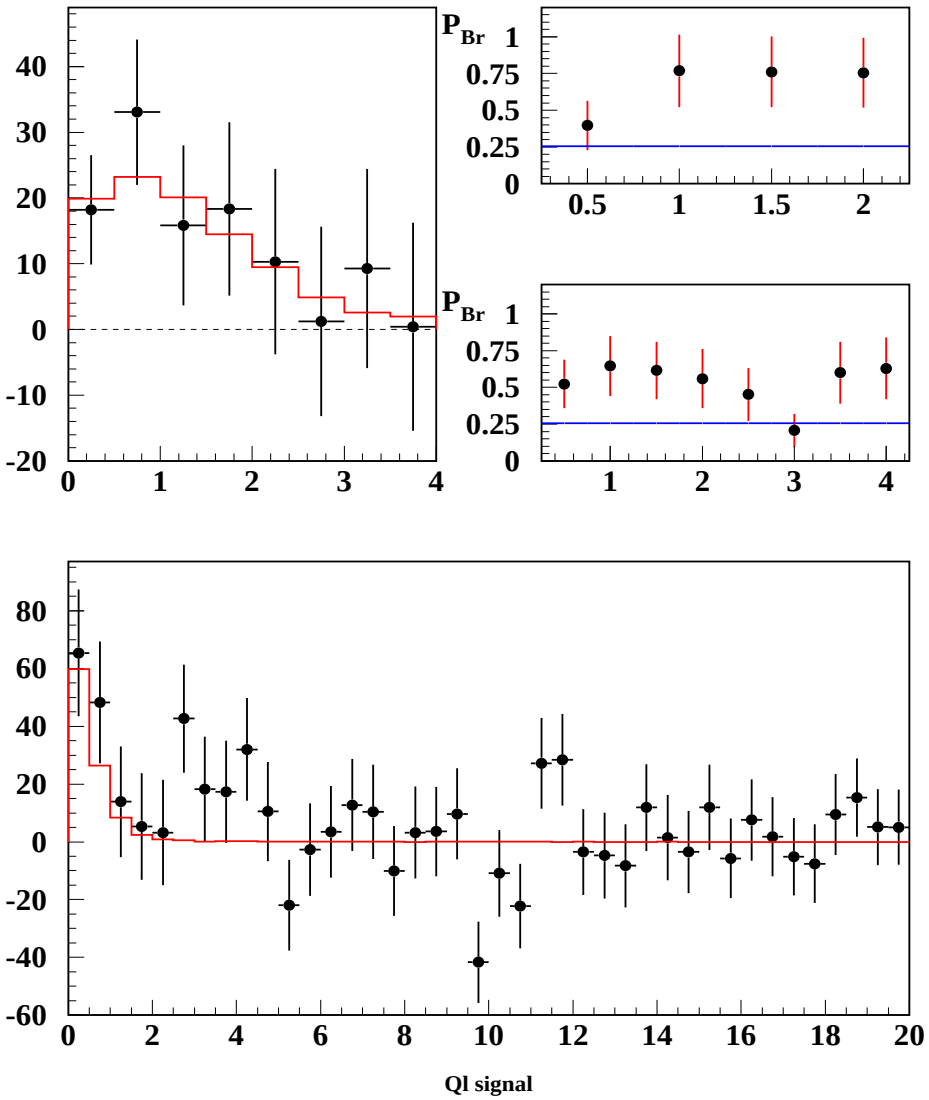

Fig. 20. *Fit results for the* $\pi^+\pi^-$ *momentum interval* $8.0 < p < 8.6$ *GeV/c in lab-frame. Caption is identical to figure 11 for the rest.*

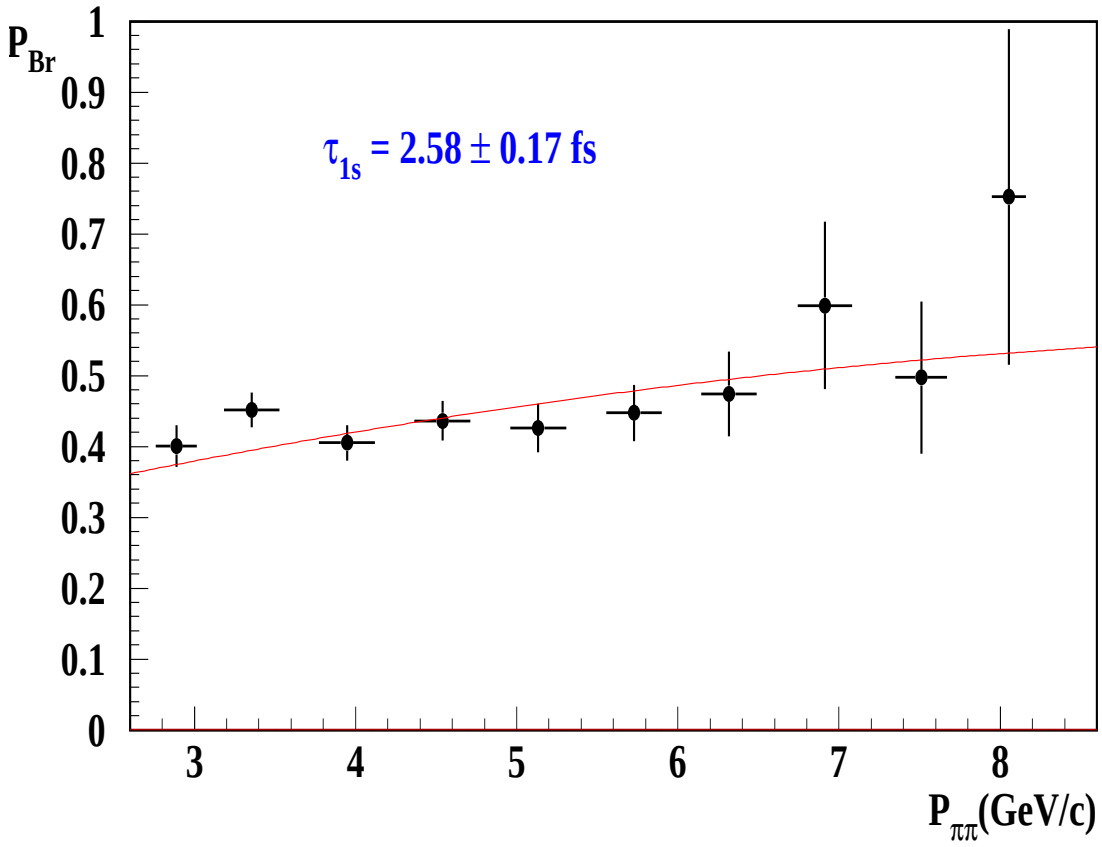

Fig. 21. *Pionium break-up probability P_{Br} as function of atom momentum, as compared to best fit Monte Carlo prediction. The fit χ^2 is 9.6 for 9 degrees of freedom. Pionium* 1*s lifetime value and error are indicated , for 2001+2002+2003 data.*

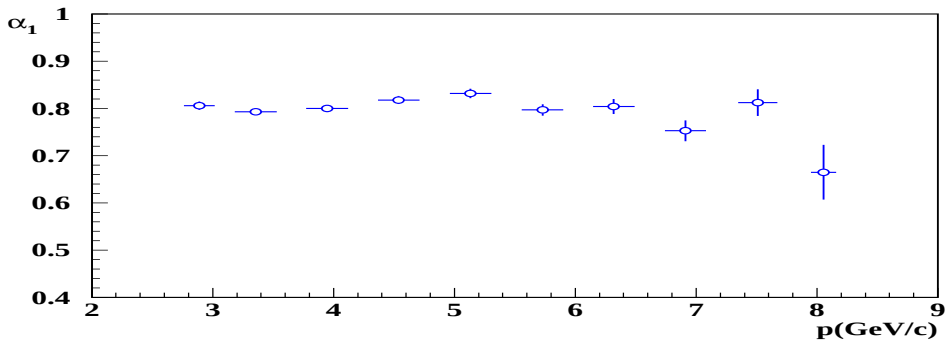

Fig. 22. *Fitted values of α_1 parameter as function of $\pi^+\pi^-$ momentum.*

The number of atom pairs N_A determined as function of p is plotted in figure 23 along with the number of Coulomb pairs given by the fit in each bin. It is seen that atom production follows rather closely the spectrum of semi-inclusive $\pi^+\pi^-$ differential cross-section, as expected from bound state production. Note that both of these spectra are uncorrected for spectrometer acceptance.

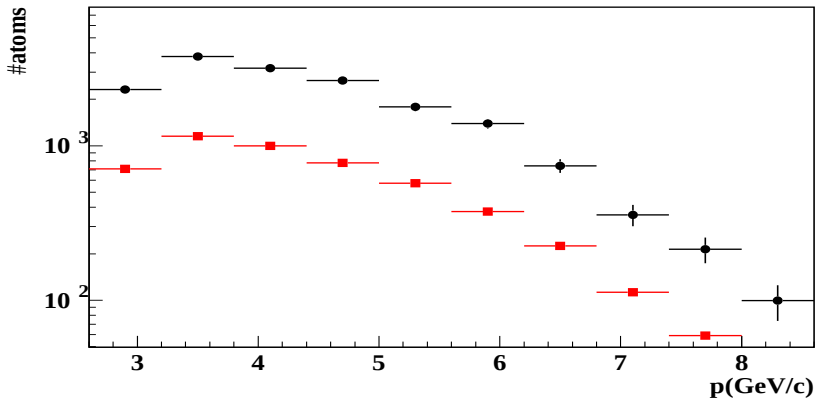

Fig. 23. *Fitted number of atom pairs as function of their lab-frame momentum (black circles) , as compared to the fitted number of Coulomb pais for $Q_L > 2MeV/c$ (coloured rectangles). The latter were normalized to half the area, to avoid the very large difference in actual scale.*

Pionium break-up probabilities can now be determined using the momentum-dependent K-factors and they are shown in figure 21. Errors were propagated from those provided by the fit for N_A and N_C. P_{Br} values are compatible with a smooth increase with increasing atom momentum, as predicted by Monte Carlo tracking inside the target foil [8] [9]. We generate a continuous set of $P_{Br}(p)$ curves with varying values of the $1s$ Pionium lifetime (τ_{1s}). χ^2 minimization with respect to this set provides a measurement of τ_{1s} and an error.

The fitted values of α_1 parameter (fraction of Coulomb pairs) are also indicated in figure 22 as function of p. They show a smooth behaviour.

In figure 24 we plot the number of non-Coulomb pairs determined by the fit as function of p, after subtraction of accidentals (as in [7],[1]), and we compare the spectrum with that previously determined for Coulomb pairs (in figure 23). The non-Coulomb spectrum is significantly softer than the Coulomb spectrum, probably due to parent multibody decays of the acompanying long-lifetime particle.

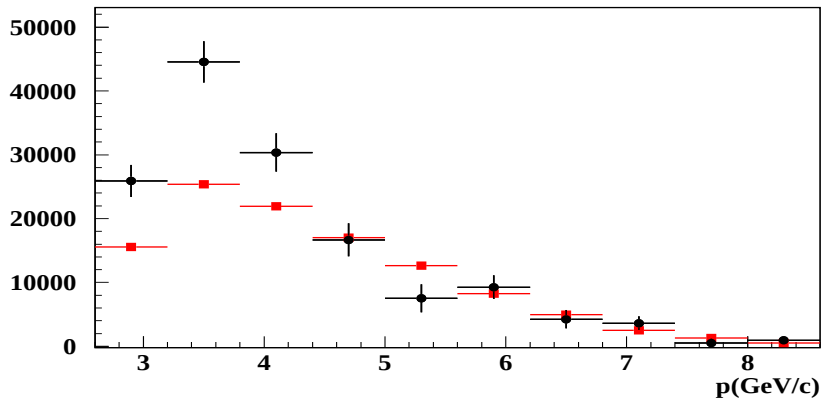

Fig. 24. *Fitted number of long-lifetime pairs (circles), determined from α_3 parameter, as function of $\pi^+\pi^-$ momentum. It is compared with the number of Coulomb pairs in figure 23 (dotted line), normalized to the same area.*

4 Systematic error

The assesment of systematic errors reported in our previous publication for 2001 data (see section 5 and summary table 12 of note [1]), remains valid with the new 2002 and 2003 data. A fundamental ingredient to this analysis has been the 1.5% study of multiple scattering in upstream detectors [10]. At least we can say there is no reason to think that any of the estimated error contributions are now larger. On the contrary, there are some indications that the new data are probably subject to smaller systematic errors, such as:

- the improved quality of the Q_T spectrum, as a consequence of two newly constructed MSGC/GEM detector planes, and one extra SFD U-plane
- larger statistics of accidental pairs, to better describe the Q_L acceptance

We therefore stick to the systematic error estimation $\Delta P_{Br} = \pm 0.006$ for the break-up probability measurement, as representative for the full DIRAC data sample.

5 Lifetime and $|a_0 - a_2|$ measurement

Pionium break-up probability P_{Br} in the Ni foil has been determined in two different ways. One is making a global (momentum-integrated) fit, which provides a single measurement for the average P_{Br}, and another is making 10 independent experiments to measure this quantity in $600 MeV/c$ wide intervals of Pionium momentum. The results (see tables 2 and 5) are in very good agreement with each other when the average P_{Br} values are compared, and have equal statistical errors. Both of them provide a high quality fit with respect to the Monte Carlo hypothesis, in terms of χ^2 probability. From each of them we can determine the Pionium $1s$ lifetime, using the standard Pionium propagation code inside the foil.

From the p-dependent fit in table 5, with the systematic error estimated in section 5, we have :

$$P_{Br} = 0.432 \pm 0.010\ (stat) \pm 0.006\ (syst)$$

or having both error sources in quadrature:

$$P_{Br} = 0.432 \pm 0.0117$$

Using the relationship between P_{Br} and lifetime obtained from the Pionium propagation code [8] [9], we determine the Pionium $1s$ lifetime from the full DIRAC data sample :

$$\tau_{1S} = 2.58\ ^{+0.19}_{-0.18}\ fs$$

where the error includes both statistic and systematic sources. It can be converted into a measurement of the difference of s-wave scattering lengths:

$$|a_2 - a_0| = 0.279 \pm 0.010\ M_\pi^{-1}$$

by means of the expression [11]:

$$\Gamma_{1s} = \frac{1}{\tau_{1s}} = \frac{2}{9}\alpha^3 p\ |a_2 - a_0|^2 (1+\delta)\ M_\pi^2$$

where $\delta = (5.8 \pm 1.2) \times 10^{-2}$ and $p = \sqrt{M_{\pi+}^2 - M_{\pi 0}^2 - (1/4)\alpha^2 M_{\pi+}^2}$.

6 Acknowledgements

We thank Cibrán Santamarina for help in utilization of his propagation code, and also Valery Yazkov, Mikhail Zhabitsky and Juan J. Saborido for their indications.

This publication would not have been possible without the strong support of Centro de Supercomputación de Galicia (CESGA), which we would like to thank very specially. In particular Carlos Fernández Sánchez, in charge of the SVGD cluster at CESGA.

The construction of this experiment was funded in part by the spanish National Program for Particle Physics from Ministerio de Educación y Ciencia (MEC), under projects FPA2005-06441, AEN99-0488 and AEN96-1671, and also by the Xunta de Galicia under projects PGIDIT06PXIB206100PR and PGIDT00PXI20602PR. We also acknowledge the support received from Xunta the Galicia as "grupo de referencia competitiva" reference 2007/000062-0.

References

[1] DIRAC Note 07-07: Final Results for Pionium Lifetime Measurement with 2001 Data, A. Romero, B. Adeva, J. L. Fungueiriño, O.Vázquez Doce.

[2] DIRAC Note 05-19: Addendum to Full-Tracking Resolution in DIRAC with 2001 Data, B. Adeva, A. Romero and O. Vázquez Doce.
DIRAC Note 05-15: Full-Tracking Resolution in DIRAC with 2001 Data, B. Adeva, A. Romero and O. Vázquez Doce.

[3] DIRAC Note 07: Pionium Lifetime Measurement with DIRAC 2002 and 2003 Ni Data, A. Romero, B. Adeva, J. L. Fungueiriño, O.Vázquez Doce, submitted at the same time as the present note

[4] DIRAC note 06-05 : Experimental Measurement of a K^+K^- Signal at $p = 2.9GeV/c$ in Ni 2001 Data, B. Adeva, A. Romero and O. Vázquez Doce.

[5] DIRAC note 07-02 : Study of $K^{\pm}\pi^{\mp}$, K^+K^- and K^-p production in DIRAC using time-of-flight measurements , B. Adeva, A. Romero and O. Vázquez Doce, C. Mariñas, J. L. Fungueiriño.

[6] DIRAC report "DIRAC targets", by A. Kuptsov, 5 March 2005.

[7] DIRAC Note 06-03: Measurement of pionium lifetime, B.Adeva, A.Romero, O.Vazquez Doce.

[8] DIRAC note 04-02: DIRAC events generator, C. Santamarina.

[9] C. Santamaria, M. Schuman, L.G. Afanasyev, T. Heim, A Monte-Carlo Calculation of the Pionium Breakup Probability with Different Sets of Pionium Target Cross Sections, J. Phys. B. At. Mol. Opt. Phys. 36 4273 (2003), arXiv:physics/0306161 v1.

[10] DIRAC Note 05-16: Study of Multiple Scattering in Upstream Detectors in DIRAC, B. Adeva, A. Romero and O. Vázquez Doce.

[11] J. Gasser, V.E. Lyubovitskij, A. Rusetsky, A. Gall, Phys. Rev. D 64 (2001) 016008, hep-ph/0103157.